



Stability Analysis of Microgrid with Load Shedding Scheme using RTDS

J. Sreedevi*, S. Vishal Kaushik and Vimalraj

Power Systems Division, Central Power Research Institute, Bengaluru – 560080, Karnataka, India; sreedevi@cpri.in

Abstract

A microgrid system was simulated using the powerful RTDS simulator; the modelling was done on the RSCAD software, and the microgrid comprised of a diesel generator, a photovoltaic (PV) system and a Doubly-Fed Induction Generator (DFIG) wind turbine system as DERs. The paper comprises the study on stability analysis of the microgrid in grid-connected and islanded modes of operation, along with a successful load shedding scheme which was implemented based on the loads distinguished as low priority and high priority loads in order to keep the system balanced during faults.

Keywords: Average Value Model (AVM), Distributed Energy Source (DER), Load Shedding, Microgrids (MG), Rate of Change of Frequency (ROCOF), Real-Time Simulation, Renewable Energy Resources (RES)

1. Introduction

Microgrids are small clusters of power generation, storage, and loads that work with the grid or independently. This technology has provided a new technical approach to the large-scale integration of renewable energy and distributed generation¹. As a key building block of a smarter grid scheme, MG has the potential to improve the utilization efficiency of energy cascade and improve power-supply reliability and power quality. Energy is considered a key input for the economical development of a country. Currently, due to the depletion of available conventional resources and concerns about environmental degradation, renewable sources such as Solar PV and Wind energy are being used to meet the everyday increasing energy demand. The conventional power grid with centralized generation is evolving to include small-scale distributed energy resources and loads connected as MG². They offer benefits such as increased use of renewable energy sources to reduce CO₂ emissions from fossil fuels, increases power supply reliability during power outages and raises revenue for the sale of energy and ancillary grid services, it is also used to provide affordable electricity to remote areas that lack power grid infrastructure. Recent experience shows that MG can improve the energy source by supplying services such as health care and telecommunications, as

well as system restoration during natural catastrophes that inflict widespread damage to power transmission grids. The growing use of DERs alters the dynamics and operation of the traditional grid. To ensure power quality and reliability, the power provided by DERs integration must be delivered to consumers within acceptable limits of current, voltage, and frequency³. The traditional distribution systems and their methods for voltage regulation and protection will no longer be effective as power flow directions vary due to the availability of DERs or fluctuations in energy sources like wind and solar radiation⁴. MGs could play a viable role in ensuring rapid and widespread integration of RES into distribution grids by providing flexible backup generation and by addressing the prevailing technical constraints. But MG is rejected due to the higher capital costs of renewable energy resources and cannot be used for stand-alone purposes to supply reliable power to critical loads when power from the utility grid is interrupted, hence this paper studies how this problem can be tackled with the help of a diesel generator as a part of the MG. The approach for stability analysis in terms of classification, operating mode, types of disturbance and time frame is discussed in this work. The development of comprehensive control systems to assure efficient, stable, and reliable operation is a key difficulty in the implementation of MG⁵. The

*Author for correspondence

RTDS simulator was used to build a real-time simulation model of a MG with DER'S, such as DG, PV system and wind system. The 7 loads modelled are also categorized based on their priority for load shedding designed in this work^{6,7}. The steady-state and transient behaviour of the MG is observed to perform satisfactorily in both grid-connected and islanded operation modes. Whereas the load-shedding scheme and the resynchronization schemes were also established successfully.

1.1 Real-Time Digital Simulation

Power system modelling tools have played a long-standing role in analysis, research and equipment development with the growing penetration of MGs and DERs. Simulation and testing have become more critical in maintaining the security and reliability of power systems than ever before⁸. However, traditional simulation and testing practices can create great difficulties for MG integration today. This is where real-time simulation comes into action, the RTDS simulator uses dedicated parallel processing hardware to run a highly detailed electromagnetic transient simulation of the power system in real-time^{9,10}. The RTDS modelling software RSCAD has extensive power system component libraries for simulating the network lines, transformers, machines, dynamic loads, DERs, power electronic converters, individual control components, and fault and breaker models^{11,12}. The unique advantage of real-time simulators is to perform hardware in-loop testing where real physical devices can be integrated into the simulated network in a closed loop¹³. Hardware in loop testing not only responds to the network conditions but also offers insight into the dynamic response of the network for any malfunction of the device¹⁴.

2. Modeling of the DERS

2.1 Diesel Generator System

It is modelled as a synchronous machine of 3MW capacity with a diesel engine excitation system and a governor which controls the speed of the shaft and the frequency of the machine as shown in Figure 1. In grid-tied operation, the generator works in speed droop mode and delivers the required reference power with respect to the grid's frequency. During the islanded operation state the DG maintains a constant frequency by switching to its isochronous mode of operation. An additional signal V_{pss} is provided to stabilize the generator's excitation system by the PSS making it accurate.

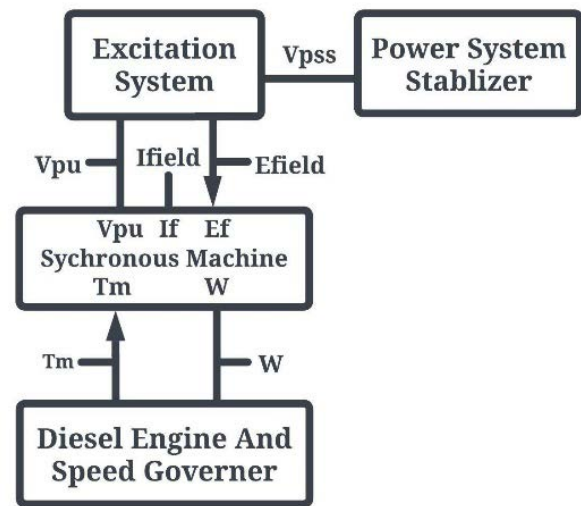


Figure 1. Model of the diesel generator.

2.2 PV- Energy System

The system in Figure 2 has a capacity of 1.74 MW along with a single-stage two-level DC/AC Voltage Source Converter (VSC). It converts the direct current of the PV array into alternating current that is injected into the grid. The system comprises Maximum Power Point Tracking to achieve maximum performance. In order to efficiently reduce the harmonics developed by the converter, smoothing filters are equipped for the purpose of grid integration. Figure 3 represents a decoupled current control technique that supports the exchange of active and reactive power between the PV system and the grid, current mode control protects the VSC from extreme current conditions and provides a strong dynamic response to any transient event. AC side voltages and currents are converted to a dq reference frame using a Phase Locked Loop (PLL) that tracks the frequency and angle of the AC voltage at the PCC of the PV system. The decoupled current controller provides the dq modulation indices m_d and m_q , which are converted into three-phase sinusoidal signals, which generate the firing pulses of the VSC.

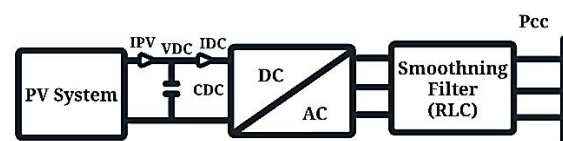


Figure 2. Single-stage, grid-connected PV system.

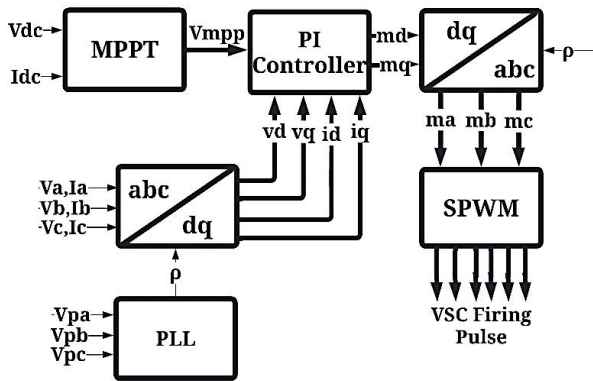


Figure 3. PV system control.

2.3 Wind Energy System

It is modelled as a Double-Fed Induction Generator (DFIG), which has a capacity of 2 MW. The rotors and blades of wind turbines capture kinetic energy and convert it into mechanical energy. The rotor side of the DFIG is connected to the grid via two-stage back-to-back VSCs with a common capacitive DC link, while the stator side is connected directly to the grid. With a power rating of around 25-30% of the total DFIG wind turbine as shown in Figure 4, the Grid-Side Converter (GSC) and Rotor-Side Converter (RSC) manage the power transferred between the wind turbine and the grid. This results in a reduced power loss of the converter and improves efficiency.

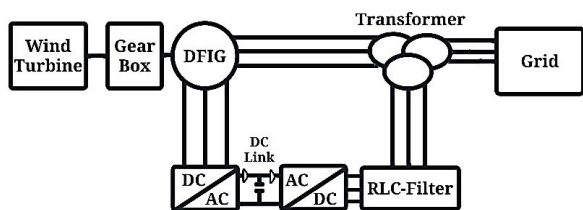


Figure 4. DFIG wind energy system.

3. Microgrid Test System

The MG is integrated into the grid through 138/13.2 kV transformer by a static switch (S1). The MG has three DERs namely PV system, a wind system and a DG as displayed in Figure 5. The DG is integrated into the MG at Bus-B7 and regulates the MGs frequency during stand-alone operation. The PV system of 1.74MW is integrated into the MG at Bus-B3 and the 2MW DFIG wind system is connected to Bus-B5. These two renewable DERs operate in a constant PQ mode to provide power during the MGs grid-connected and islanded conditions.

The system is also equipped with three switched capacitor banks with a rating of 0.5MVAR to support reactive power and facilitate resynchronization of the MG. The system has 7 loads where loads 1-4 are represented as low priority loads and loads 5-6 are represented as high priority loads. During load shedding, the loads with high priority are kept active while the loads with low priority are shed to restore system stability in the stand-alone operation mode of MG.

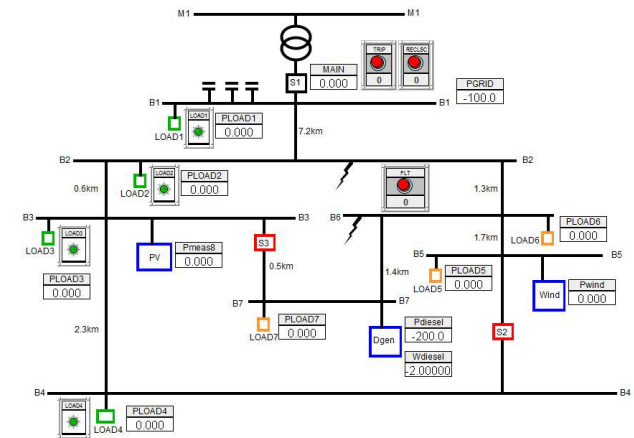


Figure 5. SLD of the microgrid.

3.1 Steady State Analysis

During the steady-state analysis, the active and reactive power generation from the DERs and absorption by loads in the microgrid under the grid-connected and stand-alone mode of operation are observed through power load flow studies.

3.1.1 Grid Connected Mode

Simulation of MG is carried out in grid-tied mode by interfacing to the utility grid, it remains stable with all its loads being fed constantly. The active and reactive power outputs of DERs and grid are provided in Table 1 along with connected loads.

Table 1(a). Output of generation sources

SOURCES	ACTIVE POWER (P in MW)	REACTIVE POWER (Q in MVAR)
PV	1.700	0.00
DG	3.012	1.58
WIND	1.975	-0.5
GRID	7.382	3.674

Table 1(b). P & Q of loads in Grid-connected mode

LOAD	ACTIVE POWER (P in MW)	REACTIVE POWER (Q in MVar)
LOAD-1	1.343	0.650
LOAD-2	0.975	0.320
LOAD-3	0.866	0.419
LOAD-4	0.885	0.428
LOAD-5	0.998	0.327
LOAD-6	1.093	0.359
LOAD-7	0.998	0.328
TOTAL	7.158	2.831

The total generation is 14.069 MW and 4.754MVar whereas the overall load consumption is 7.158 MW and 2.831 MVar during the grid-tied mode of the microgrid system.

3.1.2 Islanded Operation Mode

The MG is separated from the utility network by opening the switch S1. The diesel generator obtains its signal and changes its operation to isochronous frequency control mode and it is observed that loads 5-7 are being fed constantly, whereas drop is observed in the active power and reactive power of loads 1-4 as there is no real and reactive power supplied by the grid. The output from DERs and load consumption are provided in Table 2.

Table 2(a). Output of generation sources.

SOURCES	ACTIVE POWER (P in MW)	REACTIVE POWER (Q in MVar)
PV	1.700	0.00
DG	3.012	4.08
WIND	1.999	0.00

Table 2(b). P & Q of loads in islanded-mode

LOAD	ACTIVE POWER (P in MW)	REACTIVE POWER (Q in MVar)
LOAD-1	1.074	0.521
LOAD-2	0.858	0.282
LOAD-3	0.761	0.368
LOAD-4	0.778	0.377
LOAD-5	0.998	0.327
LOAD-6	1.093	0.359
LOAD-7	0.998	0.328
TOTAL	6.560	2.562

It is important to note that the load-shedding scheme is not activated as the loads are fed by the DERs in the MG and the diesel generator regulates the MG to a frequency of 60 Hz in isochronous mode thus keeping it stable.

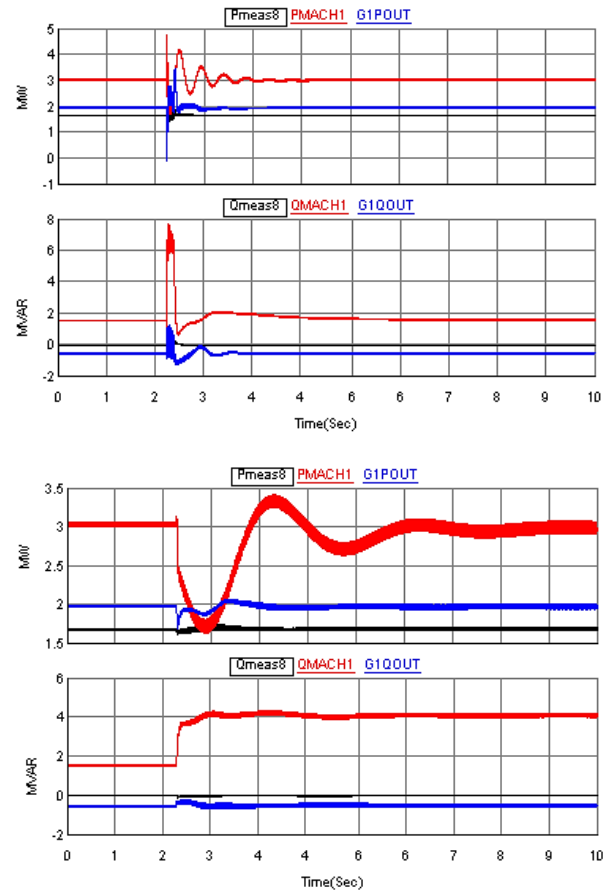


Figure 6. P and Q from PV, DG and wind during islanding.

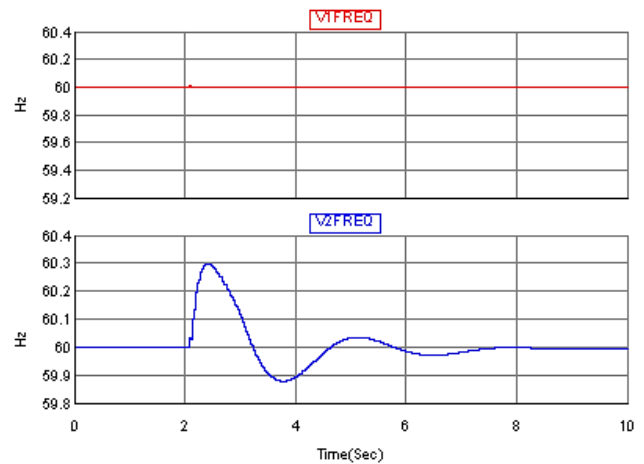


Figure 7. Frequency of (a) main grid (b) microgrid during islanding

The total DER generation is 6.782 MW and 4.08MVAR whereas the total load consumption is 6.56 MW and 2.562 MVAR in the MG system during the islanding mode of operation. The P & Q response from the generators is provided in Figure 6 for islanding operation whereas the frequency response of the main grid and microgrid are given in Figure 7.

3.2 Transient Analysis

Transient stability analysis is verified for the MG system by creating a 3-phase to-ground fault at Bus-B6 for a duration of 100 ms.

3.2.1 Transient Analysis During Grid-Connected Mode

In the grid-connected mode fault is applied at Bus-B6 and the system stability is monitored, it is observed that the fault has no effect on the MG during the grid-connected mode of operation. Active and reactive power variations of DERs for the fault at Bus-B6 are given in Figure 8. It is observed that the system remains stable after the disturbance. It is observed that the frequency of the main grid and MG has a fluctuation during the fault this can be seen in Figure 9.

3.2.2 Transient Analysis in Islanded Operation Mode

A 3-phase to ground fault is applied at Bus-B6 of the islanded MG. As the MG experiences a fault during the stand-alone condition, a power imbalance is created between the loads and the DERs power generation, which leads to a frequency fluctuation. In order to avoid the

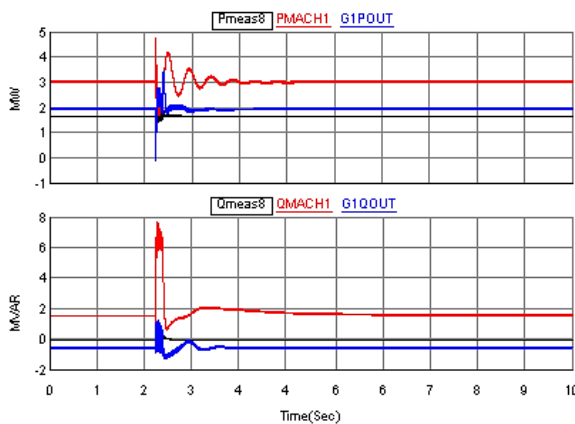


Figure 8. P and Q from PV, DG and wind in grid-connected mode during a fault.

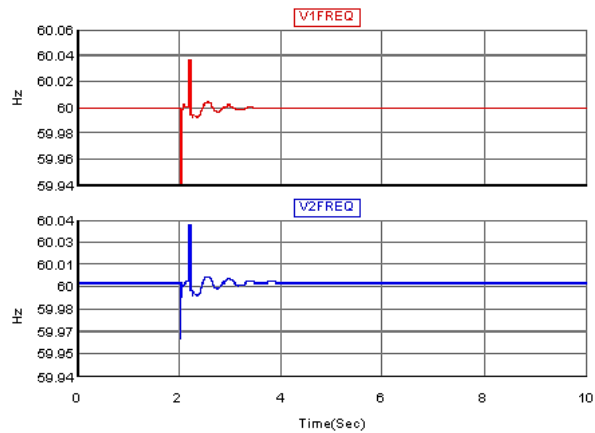


Figure 9. Frequency (a) of main grid (b) microgrid in grid-connected mode during a fault.

MG from collapsing, it has to be equipped with a quick and effective load-shedding scheme. Every scheme is designed with the consideration of loads to be shed. The load shedding occurs in stages according to their load size, threshold frequency and ROCOF. Table 3 shows the frequency criteria of the load-shedding scheme.

Table 3. load shedding scheme

Stages	Criteria for low priority loads to be shedding	Time (Sec)	Load Shed
1	$f \leq 59.5 \text{ Hz}$ or $\frac{\Delta f}{\Delta t} > \frac{3}{2} \text{ Hz}$	0.1	Load 1
2	$f \leq 58.5 \text{ Hz}$ or $\frac{\Delta f}{\Delta t} > \frac{3}{2} \text{ Hz}$	0.08	Load 2
3	$f \leq 58.3 \text{ Hz}$	0.08	Load 3
4	$f \leq 58.0 \text{ Hz}$	0.08	Load 4

The MG modelled has loads that are divided into two types namely, loads with high priority and loads with low priority, loads 1-4 are modelled as switched RL passive loads and considered as low priority loads, whereas loads 5-7 are modelled as non-switchable dynamic loads and considered as high priority loads. During a fault to keep the system stable, the loads with low priority are shed, and the loads with high priority are kept powered. After the fault is induced the load shedding scheme is activated as the ROCOF exceeds 1.5 Hz/secs, and loads 1-4 are shed to restore the frequency of the islanded MG. Table 4 shows the updated values of loads after the load shedding in the islanded MG.

Table 4. P & Q of loads after load shedding

LOAD	ACTIVE POWER (P in MW)	REACTIVE POWER (Q in MVar)
LOAD-1	0	0
LOAD-2	0	0
LOAD-3	0	0
LOAD-4	0	0
LOAD-5	1.030	0.336
LOAD-6	1.122	0.356
LOAD-7	1.643	0.342
TOTAL	3.795	1.034

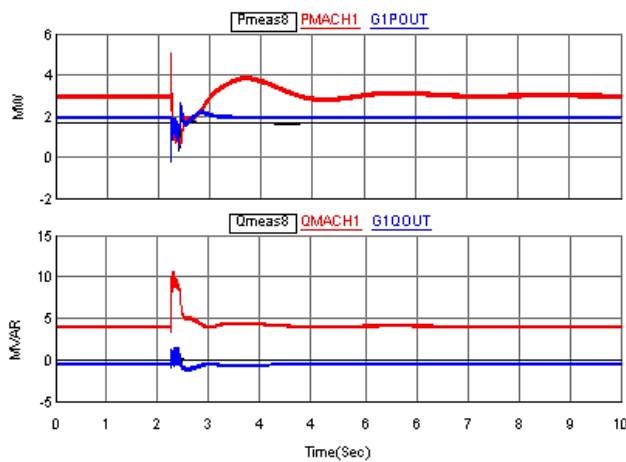


Figure 10. P and Q from PV, DG and wind in islanded mode during a fault.

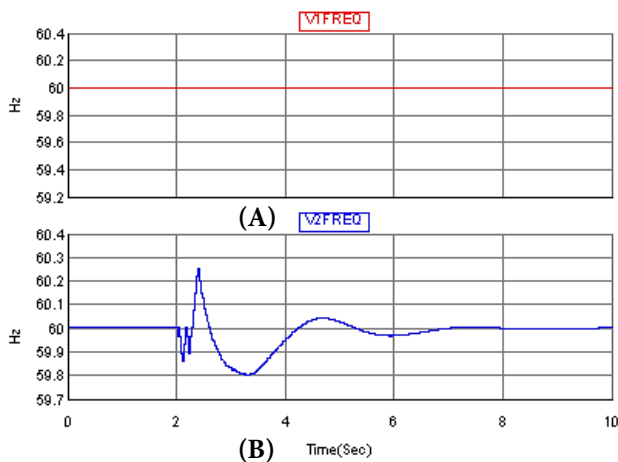


Figure 11. Frequency (a) of main grid (b) microgrid during fault in the islanded mode.

It is observed that the system remains stable after the disturbance. Active and reactive power variations of DERs for the fault at Bus-B6 are given in Figure 10. It is also observed that the frequency of the main grid is undisturbed whereas the MG has a variation during the fault but it is settled after 2.5 seconds and this can be seen in Figure 11.

4. Conclusions

This paper presents the simulation of the MG system consisting of PV, DFIG wind generator and DG is simulated. The performance of the MG in grid-connected mode and Islanding mode is analyzed during steady state and transients. When the MG system is islanded from the utility grid the modelled DG generator smoothly switches over from droop control mode to isochronous mode to maintain the frequency of the MG. When the transients occur in the MG during islanded operation to maintain stability, the load shedding scheme is implemented to shed the non-critical loads based on the frequency and ROCOF. The results prove the reliability and efficiency of the MG in every operating mode and the load shedding scheme enhances to be a rapid method to keep the system stable and remains to be highly economical for practical applications.

5. References

1. Prabaksorn T, Naayagi RT, Lee SS. Modelling and simulation of microgrid in grid-connected mode and islanded mode. 2nd International Conference on Electrical, Control and Instrumentation Engineering (ICECIE); 2020. p. 1-8. <https://doi.org/10.1109/ICECIE50279.2020.9309649>
2. Chowdhury S, Chowdhury S, Crossley P. Microgrids and active distribution networks. London: The Institution of Energy and Technology; 2009. <https://doi.org/10.1049/PBRN006E>
3. Ganjian-Aboukheili M, Shahabi M, Shafiee Q, Guerrero JM. Seamless transition of microgrids operation from grid-connected to islanded mode. IEEE Trans Smart Grid. 2020; 11(3):2106-2114. <https://doi.org/10.1109/TSG.2019.2947651>
4. Reddy GVS, Sekhar KSR, Chaudhari MA. Seamless transition of grid-connected and islanded modes in AC microgrid. IEEE First International Conference on Smart Technologies for Power, Energy and Control (STPEC); 2020. p. 1-6. <https://doi.org/10.1109/STPEC49749.2020.9297697>

5. Kundur P. Power system stability and control. New York: McGraw- Hill; 1994.
6. Gao H, Chen Y, Xu Y, Liu C-C. Dynamic load shedding for an islanded microgrid with limited generation resources. *IET Gener Transm Distrib.* 2016;10(12):2953-61. <https://doi.org/10.1049/iet-gtd.2015.1452>
7. Karimi M, Wall P, Mokhlis H, Terzija V. A new centralized adaptive under frequency load shedding controller for microgrids based on a distribution state estimator. *IEEE Trans power deliv.* 2017; 32(1):370-80. <https://doi.org/10.1109/TPWRD.2016.2594866>
8. Guillaud X, *et al.* Applications of real-time simulation technologies in power and energy systems. *IEEE Power Energy Technol.Syst J.* 2015; 2(3):103-15. <https://doi.org/10.1109/JPETS.2015.2445296>
9. Noureen SS, Roy V, Bayne SB. An overall study of a real-time simulator and application of RT-LAB using MATLAB simpowersystems. *IEEE Green Energy and Smart Systems Conference (IGESSC)*; 2017. p. 1-5. <https://doi.org/10.1109/IGESC.2017.8283453>
10. Peralta J, Saad H, Denetiere S, Mahseredjian J. Dynamic performance of average-value models for multi-terminal VSC-HVDC systems. *Power and Energy Society General Meeting. IEEE, San Diego, CA; 2012 Jul 22-26.* <https://doi.org/10.1109/PESGM.2012.6345610>
11. Ramabhotla S, Bayne SB. Modeling of energy sources in microgrid using RSCAD/RTDS. *American Journal of Advanced Research.* 2019; 3(2):7-19.
12. Peralta J, Saad H, Denetiere S, Mahseredjian J. Dynamic performance of average-value models for multi-terminal VSC-HVDC systems. *Power and Energy Society General Meeting. 2012 IEEE, San Diego, CA; 2012 Jul 22-26.* <https://doi.org/10.1109/PESGM.2012.6345610>
13. R. Technologies. RTDS Manuals and Documentation. Winnipeg; 2009. Available from: www.rtds.com.
14. Iracheta-Cortez R, Flores-Guzman N. Developing automated hardware-in-the-loop tests with RTDS for verifying the protective relay performance. *IEEE 36th Central American and Panama Convention (CONCAPAN XXXVI)*; 2016. p. 1-9. <https://doi.org/10.1109/CONCAPAN.2016.7942388>